Estimation of azimuthal angle of S-wave anisotropy using virtual cross-dipole data generated by the Virtual Source Method

Yusuke WATANABE[1], Hitoshi MIKADA[1] and Junichi TAKEKAWA[1]

[1]Dept. of Civil and Earth Res. Eng., Kyoto University

A novel scheme we proposed for analyzing S-wave azimuthal anisotropic angle in the subsurface below the seafloor has been applied to a tilted transversally isotropic medium of horizontal axis of symmetry (HTI). The proposed method utilizes the virtual source method to acquired data set with single ocean bottom seismometer and an air-gun array. To evaluate the effectiveness of our scheme, we conducted the numerical experiments for 3D model with a tilted anisotropic target. We applied this method to the synthetic data to make the virtual cross-dipole data at each shot location. Finally we applied the Alford rotation to estimate an azimuthal angle of the anisotropy of the target layer. Our numerical results show the limitations of the Alford rotation. Especially, the Alford rotation assumes that a dipole signal in one direction has an amplitude equivalent to the other dipole to the other normal direction in the cross dipole measurements. Since our approach could not assume the equality of the amplitudes for each of the cross dipole signals, we conclude that a strategy using full waveforms needs to be taken into consideration for estimating azimuthal angle of tilted targets.

1. INTRODUCTION

S-wave survey tells us the knowledge of subsurface current stress field and stress field history. This information is important for drilling design, hydraulic fracturing plan, etc. Although S-wave survey has more and more important role, offshore S-wave survey is quite challenging because of zero shear modulus of water. This difficulties to generate S-wave signal in offshore environment has prevented the practice of offshore S-wave surveys[1), 2)]. We proposed a novel scheme[3)] to estimate anisotropic information in the subsurface by utilizing the virtual source method[4)] to overcome the problem alluded in the above. In our previous study[3)], the proposed method demonstrated its effectiveness in the application of the Alford rotation[5)] to virtual traces were generated for data acquired by an tri-component ocean bottom seismometer for a series of air-gun shooting. The next step is to extend our methodologies to more realistic or complex models.

In the application of the proposed method, we may need to recall that the Alford rotation may fail to estimate the direction of axis of symmetry for a titled TI medium[6)] due to the convergence in the minimization procedure. Also, our virtual source approach may results in the generation of cross dipole traces in the right angle with a considerable difference in the amplitudes. Before any detailed discussion, the limitations of the Alford rotation needs to be confirmed.

In this study, we apply the proposed method to a numerical model which has a tilted target reflector with azimuthal S-wave anisotropy. Azimuthal angle of the target layer is estimated by the Alford rotation[5)] with the virtual cross-dipole data sets. We will show the numerical results and discuss the limitations of the Alford rotation. After discussion about the issues regarding the present scheme, future direction for surveying the anisotropic structure will be presented.

2. 3D SEISMIC WAVE SIMULATION

In this chapter we introduce the method to make synthetic 3D seismic data sets for our analysis.

(1) Model settings

As shown in **Fig. 1,** we set a four-layered model. We put an OBS on the seafloor in the center of the model. We define a 1200m length of survey line and set 101 shots of air-gun sources in every 12m beneath the sea surface. We use the Ricker wavelet with 10Hz dominant frequency as a source function. We use the PML absorbing boundaries to suppress artificial reflection waves from model edges. We modeled the tilted anisotropic layer as a HTI model

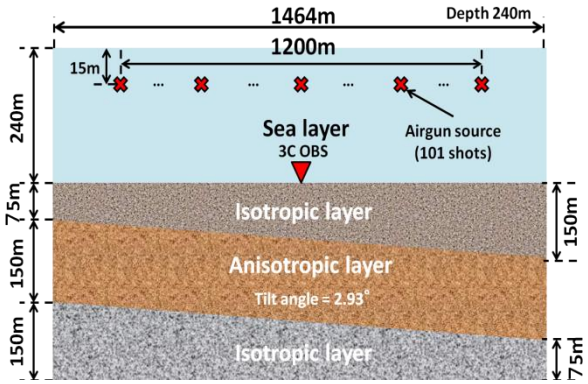

Fig. 1 Model settings

Table 1 Model parameters

Sea layer		Isotropic layer [Upper]	
ρ	1000	ρ	2200
Vp [m/s]	1500	Vp [m/s]	2700
Vs [m/s]	0	Vs [m/s]	1559
Anisotropic layer [Target]		**Isotropic layer [Below]**	
ρ	2700	ρ	2900
Vpf,Vps [m/s]	3200 2880	Vp [m/s]	3500
Vsf,Vss [m/s]	1848 1663	Vs [m/s]	2021

with azimuthal anisotropic angle of 30 and 60 degrees. The model parameter and calculation conditions are shown in **Table 1.**

(2) Received gathers

We show the common receiver gathers of each model and each component.

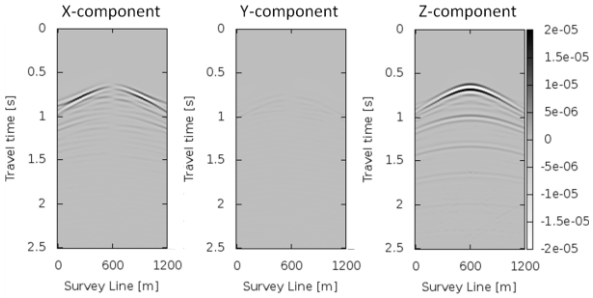

Fig. 2 Received gathers in 30deg. model

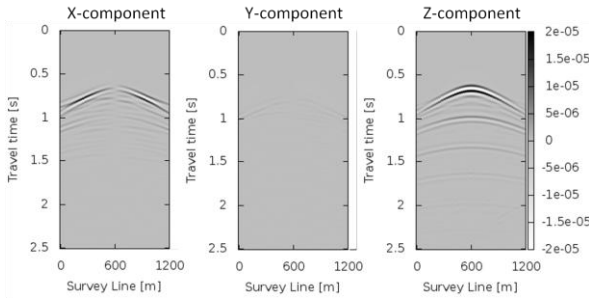

Fig. 3 Received gathers in 60deg. model

From left, it shows *x*-direction, *y*-direction and *z*-direction component of received data in each models.

3. VIRTUAL CROSS-DIPOLE DATA

In this section, we show the scheme for generating the virtual cross-dipole data and azimuthal anisotropic angle estimation. The entire analysis flowchart is shown in **Fig. 4**.

Fig. 4 Analysis flowchart

(1) Pre-filters

As pre-filter we utilized FK-filter to x-component separated data and y-component data in order to extract tilted signal from the received data. In **Fig. 5** we show the FK-filter design. In the

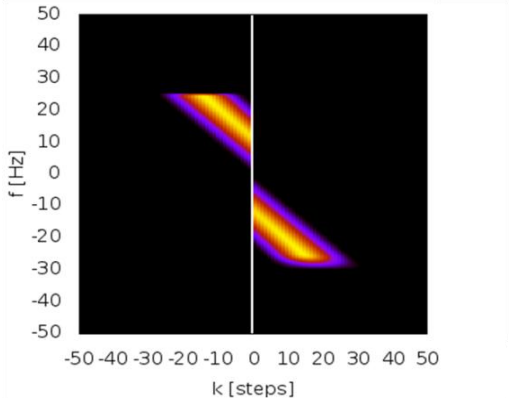

Fig. 5 FK-filter designs

figure, dark colored region spectrum is muted.

(2) Virtual Source Method to generate cross-dipole data

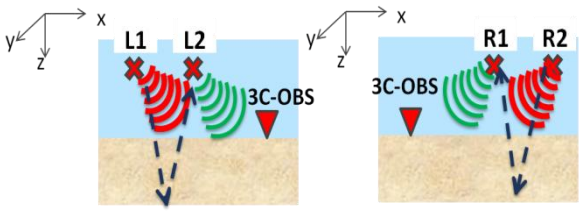

Fig. 6 Concepts of the virtual source method

By calculating cross correlation function of adjacent horizontal component received data, we generate the virtual cross-dipole data sets in each physical shot point. We virtually extract horizontal forces from air-gun's explosive forces just by making the interferogram of red lay and green lay shown in **Fig. 6**. In case of L1 and L2 source points, we use the equations below.

$$V_{xx} = V_{L1x} \otimes V_{L2x} \quad V_{xy} = V_{L1x} \otimes V_{L2y}$$
$$V_{yx} = V_{L1y} \otimes V_{L2x} \quad V_{yy} = V_{L1y} \otimes V_{L2y} \qquad (1)$$

V_{L1x} and V_{L2x} means truly received data of x-direction particle velocity from L1 or L2. $\otimes$ means cross-correlation and V_{xx} is one of components in the virtual cross-dipole data and means virtual shots in x-direction at L1 and R1, and virtually receives in x-direction at L2 and R2. In the case of R1 and R2, we use equations below.

$$V_{xx} = V_{R2x} \otimes V_{R1x} \quad V_{xy} = V_{R2x} \otimes V_{R1y}$$
$$V_{yx} = V_{R2y} \otimes V_{R1x} \quad V_{yy} = V_{R2y} \otimes V_{R1y} \qquad (2)$$

(3) Alford rotation

Finally we use the Alford rotation to estimate azimuthal angle of the target layer. The time window is set in ± 0.1s from the theoretical travel time of the virtual shear signal.

4. RESULTS

In this chapter, we show the result of the virtual cross-dipole data sets and the final results of azimuthal angle estimation.

(1) Virtual cross-dipole data sets

The virtual cross-dipole gathers are shown in **Figs. 7** and **8.** In each gathers hatches in each component shows the time we used in Alford rotation.

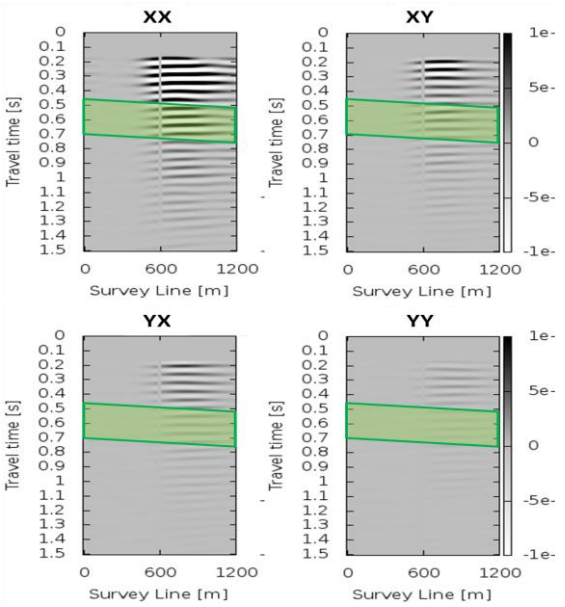

Fig. 7 The virtual 4C data in 30 deg.

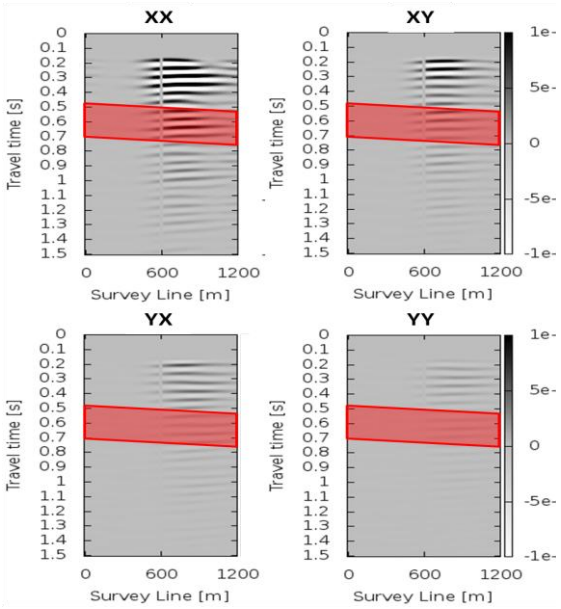

Fig. 8 The virtual 4C data in 60deg.

(2) Estimation result after Alford rotation

In this section, we show the result of Alford rotation. We show the result of 30 deg. model in **Fig. 9**, and 60 deg. model in **Fig. 10**.

In these figures each dot represents the estimation result of azimuthal angle and each dotted line shows the modeled angle.

The result shows the estimation error of the tilted layer model becomes larger than that in the case of horizontal layered model. This is because of the limitation of the Alford rotation. The detail of this limitation will be discussed in the next chapter.

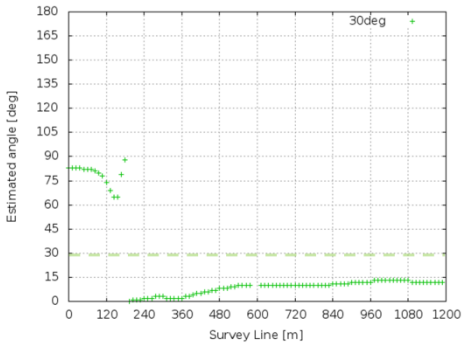

Fig.9 The final estimation result of 30 deg. model

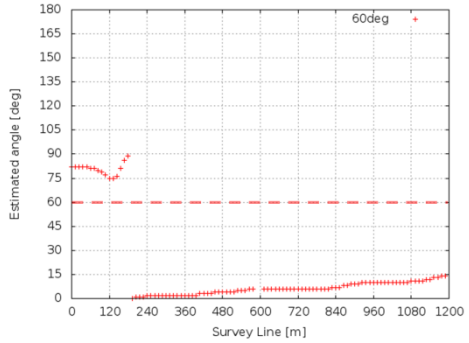

Fig. 10 The final estimation result of 60 deg. model

5. DISCUSSION AND CONCULUTION

In this study, the azimuthal angle estimation result had relatively large error. From these results, we could find some limitations of our scheme for dipped anisotropic target and hard sea floor models. One of the limitations comes from the limitation of Alford rotation to the tilted anisotropic target reported by Fuse et. al. (2016)[6]. In the paper, the accuracy of estimation is not sufficient in the case of TTI model. In our numerical experiments, we approximate the anisotropic target as HTI model. However when the target's reflection plane is dipped, it becomes apparently TTI model (shown in **Fig. 11**).

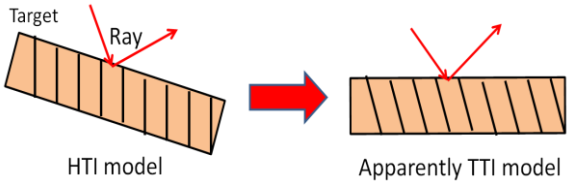

Fig. 11 Concept of the apparently TTI model

The other limitation comes from the limitation of Alford rotation to the hard sea floor model. In hard sea floor model S-wave velocity is large. Therefore S-wave has penetrated before S-wave splits sufficiently. Then the virtual cross-dipole data in V_{yy} is much weaker than the virtual source V_{xx} (see **Figs. 7** and **8**). In this case which V_{xx} extremely larger than V_{yy}, the energy distribution between components changes monotonically V_{xx} to V_{yy} (see **Fig. 12**).

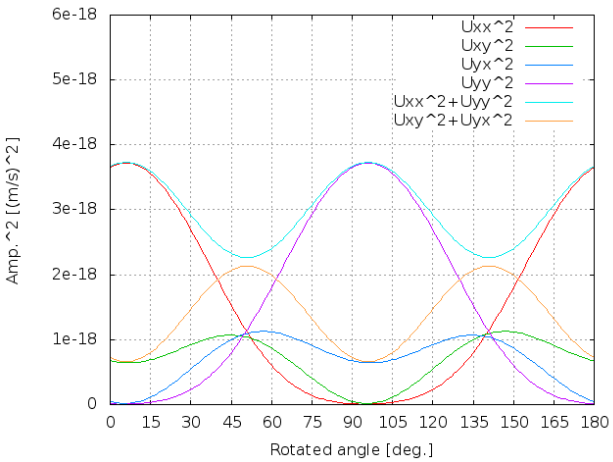

Fig. 12 Energy distribution

The reason for this energy distribution between components to component in the case of hard sea floor is possible to be explained with some approximation in Alford rotation equations (see **Appendix**).

To remove the limitations of our offshore virtual S-wave scheme, we need some additional steps in our current scheme. In Fuse et. al. (2016)[7], they proposed the new usage of full waveform inversion (FWI) to estimate the anisotropic parameters such as azimuth and dip angles with cross-dipole datasets. We would like to propose entirely new scheme combining virtual source data and FWI (shown in **Fig. 13**). By using this new scheme the limitations of our method will be removed and the offshore S-wave survey will be possible without any limitations.

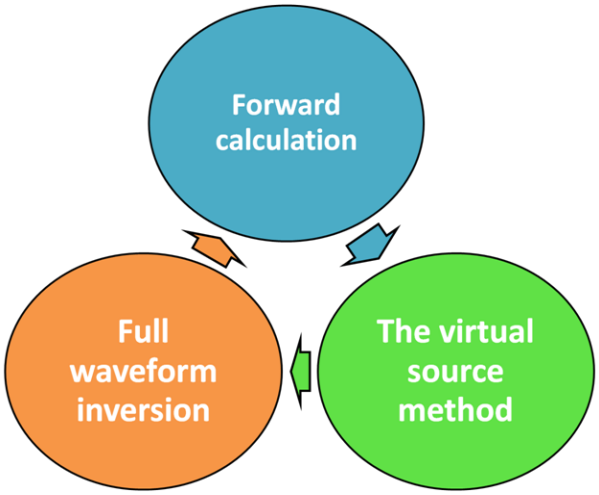

Fig. 13 The concepts for new scheme

6. CONCULUTION

In this study we conducted some numerical experiments to apply our proposed offshore S-wave survey method to tilted anisotropic target.

The result shows the estimation error is relatively larger than in the case of horizontal models. This error indicates the limitations of Alford rotation in the case which the target is tilted and the case of hard sea floor models. From these limitations we make possible to propose the new scheme which combines the Virtual Source Method and Full waveform Inversion.

REFERENCES

1) Nagai,Y., Tsuda, A., Ozasa H., Hatanaka,H., Tanaka, K., Tagami, M., Sato, F., Takekawa, J., and Mikada, H., 2016, Towed Marine Dipole Source for Shear Wave Generation: *78th EAGE Conference and Exhibition*, doi: 10.3997/2214-4609.201600861.

2) Ozasa, H., Takekawa, J., and Mikada, H., 2017, Use of Virtual Dipole Shear Source in Offshore Shear Wave Exploration without Any Contact to the Seafloor, *79th EAGE Conference and Exhibition*, doi: 10.3997/2214-4609.201701181.

3) Watanabe, Y., Mikada, H., and Takekawa, J., 2017, Estimate azimuthal shear-wave anisotropy

by applying virtual-source method with a line of air-gun shots and a single ocean-bottom seismometer. SEG Technical Program Expanded Abstracts 2017: pp. 2476-2480.
4) Bakulin, A., Mateeva, A., Calvert, R., Jorgensen, P., and Lopez, J., 2007, Virtual shear source makes shear waves with air guns: *Geophysics*, **72**, A7-A11.
5) Alford, R.M., 1986, Shear Data in the Presence of Azimuthal Anisotropy: *56th Annual International Meeting, SEG, Expand Abstracts*, 476-479.
6) Fuse, S., Mikada, H., and Takekawa, J., 2016, Waveform Disturbance by Transversely Isotropic Medium with a Tilted Axis of Symmetry around a Borehole: *The 20th International Symposium on Recent Advances in Exploration Geophysics (RAEG 2016), Expanded Abstracts*, doi: 10.3997/2352-8265.20140204
7) Fuse, S., Mikada, H., and Takekawa, J., 2016, Waveform analysis of borehole acoustic dipole data in transversely isotropic medium with a tilted axis of symmetry: *86th Annual International Meeting, SEG, Expanded Abstracts*, 667-671.

Appendix: Alford rotation equations approximation in the case of hard sea floor

Firstly the fundamental equations of Alford rotation are shown in below.

$$\mathbf{U} = \begin{bmatrix} u_{xx} & u_{xy} \\ u_{yx} & u_{yy} \end{bmatrix} = \mathbf{R}^{\mathrm{T}}\mathbf{V}\mathbf{R} \tag{3}$$

$$u_{xx} = v_{xx}\cos^2\theta + v_{yy}\sin^2\theta + 0.5\left(v_{yx} + v_{xy}\right)\sin 2\theta \tag{4}$$

$$u_{xy} = v_{xy}\cos^2\theta - v_{yx}\sin^2\theta + 0.5\left(v_{yy} - v_{xx}\right)\sin 2\theta \tag{5}$$

$$u_{yx} = v_{yx}\cos^2\theta - v_{xy}\sin^2\theta + 0.5\left(v_{yy} - v_{xx}\right)\sin 2\theta \tag{6}$$

$$u_{yy} = v_{yy}\cos^2\theta + v_{xx}\sin^2\theta - 0.5\left(v_{yx} - v_{xy}\right)\sin 2\theta \tag{7}$$

V means the received cross-dipole data matrix, **U** means rotated cross-dipole data matrix, **R** means rotation matrix and θ means rotation angle. In our model each components are approximated like below.

$$v_{xx} \gg v_{yy} \tag{8}$$

$$v_{yx} \cong v_{xy} \tag{9}$$

$$v_{xx} \cong v_{xy} \tag{10}$$

With using this approximation, diagonal component's power is calculated like below.

$$\begin{aligned}
&(u_{xx})^2 \\
&= \left(v_{xx}\cos^2\theta + v_{yy}\sin^2\theta + 0.5\left(v_{yx} + v_{xy}\right)\sin 2\theta\right)^2 \\
&\cong {v_{xx}}^2\left(\cos^2\theta + \frac{v_{yy}}{v_{xx}}\sin^2\theta + \sin 2\theta\right)^2 \\
&\cong {v_{xx}}^2\left(\frac{7}{8} + \frac{1}{2}\cos 2\theta + \sin 2\theta + \frac{1}{2}\sin 4\theta - \frac{3}{8}\cos 4\theta\right) \\
&\cong {v_{xx}}^2\left(A_{xx} + B_{xx}\cos\left(2\theta + \varphi_{xx}\right)\right) \\
&(A_{xx}, B_{xx}, \varphi_{xx} = const.)
\end{aligned} \tag{11}$$

$$\begin{aligned}
&(u_{yy})^2 \\
&= \left(v_{yy}\cos^2\theta + v_{xx}\sin^2\theta - 0.5\left(v_{yx} + v_{xy}\right)\sin 2\theta\right)^2 \\
&\cong {v_{xx}}^2\left(\sin^2\theta + \frac{v_{yy}}{v_{xx}}\cos^2\theta + \sin 2\theta\right)^2 \\
&\cong {v_{xx}}^2\left(\frac{7}{8} - \frac{1}{2}\cos 2\theta - \sin 2\theta + \frac{1}{2}\sin 4\theta - \frac{3}{8}\cos 4\theta\right) \\
&\cong {v_{xx}}^2\left(A_{yy} - B_{yy}\cos\left(2\theta + \varphi_{xx}\right)\right) \\
&(A_{yy}, B_{yy}, \varphi_{xx} = const.)
\end{aligned} \tag{12}$$

$$\begin{aligned}
&E_{diagonal} = (u_{xx})^2 + (u_{yy})^2 \\
&\cong 2{v_{xx}}^2\left(\frac{7}{8} + \frac{1}{2}\sin 4\theta - \frac{3}{8}\cos 4\theta\right) \\
&\cong 2{v_{xx}}^2\left(A_{diagonal} - B_{diagonal}\cos\left(4\theta + \varphi_{diagonal}\right)\right) \\
&(A_{diagonal}, B_{diagonal}, \varphi_{diagonal} = const.)
\end{aligned} \tag{13}$$

This approximation matches the energy rotated curve in **Fig. 12.**

Diagonal component's power is calculated like below with same approximations.

$$\begin{aligned}
&(u_{xy})^2 \\
&= \left(v_{xy}\cos^2\theta - v_{yx}\sin^2\theta + 0.5\left(v_{yy} - v_{xx}\right)\sin 2\theta\right)^2 \\
&\cong {v_{xx}}^2\left(\cos^2\theta - \sin^2\theta + 0.5\left(\frac{v_{yy}}{v_{xx}} - 1\right)\sin 2\theta\right)^2 \\
&\cong {v_{xx}}^2\left(\frac{5}{8} + \frac{5}{8}\cos 4\theta - \frac{1}{2}\sin 4\theta\right) \\
&\cong {v_{xx}}^2\left(A_{xy} + B_{xy}\cos\left(4\theta + \varphi_{xy}\right)\right) \\
&(A_{xy}, B_{xy}, \varphi_{xy} = const.)
\end{aligned} \tag{14}$$

$$\begin{aligned}
&(u_{xy})^2 \\
&= \left(v_{yx}\cos^2\theta - v_{xy}\sin^2\theta + 0.5\left(v_{yy} - v_{xx}\right)\sin 2\theta\right)^2 \\
&\cong {v_{xx}}^2\left(\cos^2\theta - \sin^2\theta + 0.5\left(\frac{v_{yy}}{v_{xx}} - 1\right)\sin 2\theta\right)^2 \\
&\cong {v_{xx}}^2\left(\frac{5}{8} + \frac{5}{8}\cos 4\theta - \frac{1}{2}\sin 4\theta\right) \\
&\cong {v_{xx}}^2\left(A_{yx} + B_{yx}\cos\left(4\theta + \varphi_{yx}\right)\right) \\
&(A_{yx}, B_{yx}, \varphi_{yx} = const.)
\end{aligned} \tag{15}$$

$$\begin{aligned}
&E_{off-diagonal} = (u_{xy})^2 + (u_{yx})^2 \\
&\cong 2{v_{xx}}^2\left(\frac{5}{8} + \frac{5}{8}\cos 4\theta - \frac{1}{2}\sin 4\theta\right) \\
&\cong 2{v_{xx}}^2\left(A_{off} + B_{off}\cos\left(4\theta + \varphi_{off}\right)\right) \\
&(A_{off}, B_{off}, \varphi_{off} = const.)
\end{aligned} \tag{16}$$

These approximated equations also match the observed energy rotation curves. By using this approximation, we are possible to explain the observed phenomenon.